Received: 6 July 2020 | Revised: 21 September 2020 | Accepted: 1 December 2020

DOI: 10.1002/jor.24936

RESEARCH ARTICLE

Journal of Orthopaedic Research®

Cartilage articulation exacerbates chondrocyte damage and death after impact injury

Steven Ayala[1] | Michelle L. Delco[2] | Lisa A. Fortier[2] | Itai Cohen[3] | Lawrence J. Bonassar[1,4]

[1]Meinig School of Biomedical Engineering, Cornell University, Ithaca, New York, USA

[2]Department of Clinical Sciences, College of Veterinary Medicine, Cornell University, Ithaca, New York, USA

[3]Department of Physics, Cornell University, Ithaca, New York, USA

[4]Sibley School of Mechanical and Aerospace Engineering, Cornell University, Ithaca, New York, USA

Correspondence

Lawrence J. Bonassar, Department of Biomedical Engineering, 149 Weill Hall, Cornell University, Ithaca, NY 14853, USA.
Email: lb244@cornell.edu

Funding information

Alfred P. Sloan Foundation; National Institutes of Health, Grant/Award Numbers: 5R01AR071394-03, S10OD018516; Harry M. Zweig Memorial Fund for Equine Research; National Science Foundation, Division of Civil, Mechanical and Manufacturing Innovation, Grant/Award Number: CMMI-1536463; New York State Stem Cell Science, Grant/Award Number: CO29155; National Science Foundation, Division of Materials Research, Grant/Award Number: DMR-1807602; National Institute of Arthritis and Musculoskeletal and Skin Diseases, Grant/Award Numbers: 1R03AR075929-01, 5K08AR068470-02

Abstract

Posttraumatic osteoarthritis (PTOA) is typically initiated by momentary supraphysiologic shear and compressive forces delivered to articular cartilage during acute joint injury and develops through subsequent degradation of cartilage matrix components and tissue remodeling. PTOA affects 12% of the population who experience osteoarthritis and is attributed to over $3 billion dollars annually in healthcare costs. It is currently unknown whether articulation of the joint post-injury helps tissue healing or exacerbates cellular dysfunction and eventual death. We hypothesize that post-injury cartilage articulation will lead to increased cartilage damage. Our objective was to test this hypothesis by mimicking the mechanical environment of the joint during and post-injury and determining if subsequent joint articulation exacerbates damage produced by initial injury. We use a model of PTOA that combines impact injury and repetitive sliding with confocal microscopy to quantify and track chondrocyte viability, apoptosis, and mitochondrial depolarization in a depth-dependent manner. Cartilage explants were harvested from neonatal bovine knee joints and subjected to either rapid impact injury (17.34 ± 0.99 MPa, 21.6 ± 2.45 GPa/s), sliding (60 min at 1 mm/s, under 15% axial compression), or rapid impact injury followed by sliding. Explants were then bisected and fluorescently stained for cell viability, caspase activity (apoptosis), and mitochondria polarization. Results show that compared to either impact or sliding alone, explants that were both impacted and slid experienced higher magnitudes of damage spanning greater tissue depths.

KEYWORDS

apoptosis, impact, mitochondria, posttraumatic osteoarthritis

1 | INTRODUCTION

Clinically, 12% of osteoarthritis is posttraumatic (PTOA) affecting approximately 5.6 million individuals in the United States and attributed to over $3 billion dollars annually in healthcare costs.[1-3] PTOA is initiated by momentary supraphysiologic shear and compressive forces created during physical trauma that results in cartilage damage and subsequent joint inflammation.[4-6] Typically, patients who develop PTOA are young, active, and have suffered some type of traumatic injury such as anterior cruciate ligament (ACL) rupture, meniscus tear, or shoulder dislocation.[4,7-10] Such patients typically require surgical intervention early in life and often

suffer rapid OA progression caused by damage to chondrocytes and/or extracellular matrix.[8,11]

There are numerous cellular responses that occur as a consequence of injury, and some, like mitochondrial (MT) pathways towards cell death, may be amenable to intervention. For mitochondria in particular, depolarization occurs minutes after injury and leads to bioenergetic failure of the cell through decreased ATP production.[12] MT depolarization also leads to increases in oxidative stress, inflammation, caspase activation and excess reactive oxygen species production, resulting in apoptosis and cell death respectively.[13,14] Studies have also shown that MT dysfunction results in decreased collagen II secretion by chondrocytes, which may increase cartilage degeneration in the pathogenesis of OA.[15] In patients with later-stage OA, chondrocytes experience downregulation of superoxide dismutase 2 resulting in increased MT DNA strand breaks as well as reduced activities of complexes II and III resulting in decreased energy production.[16,17] While mitochondrial repolarization is possible, prolonged depolarization past an unknown threshold of time leads to mitochondrial damage and depending on the severity can induce cell death by apoptosis or necrosis if the damage is extensive.[18,19] While there are promising new chemical interventions to halt the progression of mitochondrial and other biochemical processes,[20,21] the current standard of care is to prescribe rehabilitation therapy to improve supporting musculature strength, joint functionality, and decrease pain.[22-24]

It is unknown, however, if movement soon after joint injury is beneficial or detrimental to long-term outcome and the development of PTOA. Complete immobilization of knee joints has been noted to be beneficial for up to 2 weeks post-surgery by decreasing rate of apoptosis and increasing rate of proliferation.[25] However, immobilization of longer than 2 weeks or shorter than 1 week has been noted to cause further damage within the joint by increasing rate of apoptosis, decreasing rate of proliferation, and decreasing glycosaminoglycan content.[26]

Since the timeline of cartilage damage to PTOA is not fully understood, it is unclear if movement of an injured joint may further damage chondrocytes.[27] Previous work modeled initiation of PTOA in cartilage tissue through ACL transection, meniscal destabilization, delivering impact injury, or shear strain through sliding.[28-33] While each of these techniques have the potential to cause cellular injury, it is unknown if damage would be exacerbated by impact and subsequently sliding injured cartilage.[12,30-32] This type of loading modality would be possible after articulating joints that have endured falls, sports injury, or traumatic injury.[34,35] These combined mechanical forces would more closely simulate the mechanical environment of an injured joint that is subject to continued use after trauma. Based on previous work that showed sliding alone can damage tissue,[30] we hypothesize that sliding previously impacted tissue will lead to a synergistic increase in chondrocyte damage in a depth-dependent manner throughout the tissue. The results of this study will reveal what regions of the cartilage tissue are most damaged following injury and if prior injury leaves the cartilage predisposed to continued arthritic degeneration.

2 | MATERIALS AND METHODS

2.1 | Tissue harvest and preparation

Cartilage from the femoral condyles of six neonatal (i.e., skeletally immature) bovids (sex unknown; Gold Medal Packing) was harvested, rinsed with 1× Dulbecco's phosphate-buffered saline (DPBS) containing antibiotics (100 U/ml penicillin-streptomycin, Mediatech) and sectioned into cylindrical plugs using 6 mm diameter biopsy punches (Integra) using sterile practices. Explants were trimmed, while keeping the articular surface intact, to 2 mm in depth using a custom jig and blades lubricated with bovine synovial fluid (Lampire) to minimize shear force and limit chondrocyte death preceding testing. Before injury, explants were incubated overnight in media (phenol red-free DMEM containing 1% FBS, HEPES 0.025 ml/ml, penicillin 100 U/ml, streptomycin 100 U/ml, and 2.5 mM glucose) at 37°C, 5% CO_2.

2.2 | Cartilage impact protocol

Cartilage explants were subjected to injury using a previously described, spring-loaded impactor system.[29,36] A single cycle of unconfined compression was delivered to the articular surface of explants using a 12 mm diameter cylindrical impacting head. All impacts were delivered, over a loading time of ~ 1 ms, at a peak stress of 17.34 ± 0.99 MPa and peak stress rate of 21.6 ± 2.45 GPa/s (10 mm internal spring compression). While loading magnitudes of this nature have been seen in previous studies to cause failure of the anterior cruciate ligament,[37] this impacting protocol was chosen to deliver impact trauma resulting in pathological cell death without fibrillation or full thickness cracking.[5,32,38] Impact force was measured at 50 kHz using a load cell mounted in parallel to the impacting missile (PCB Piezotronics). A linear variable differential transducer (LVDT; RDP Electronics) was mounted in parallel with the impacting tip to measure the deformation of the cartilage plugs.

2.3 | Cartilage sliding protocol

Impacted and non-impacted cartilage explants were slid against a polished glass counterface (McMaster Carr) in a custom-built tribometer.[30,39] Explants were submerged in a lubricating bath of bovine synovial fluid (Lampire). Before sliding, explants were compressed to 15% axial strain and allowed to equilibrate for 60 min.[40] Some level of static compression is required for these experiments to ensure that there is not slippage between the plug and the glass counterface.[41] Our previous work has investigated a wide variety of static compressions and sliding speeds[40,42] and has shown that 15% compression followed by sliding[30] is quite reliable at producing cell death, apoptosis, and mitochondrial depolarization. Explants were slid for 60 min at 1 mm/s as actuated by a lead screw-driven stage actuated by a micro-stepper motor (MDrive Plus, Schneider Electric).[30]

2.4 | Study design

Cartilage explants were randomly assigned to one of four treatment groups ($n \geq 7$/group), uninjured control, sliding, impact, and impact followed by sliding. At time zero, explants in the sliding group were mounted onto the tribometer and allowed to stress relax for 1 h before beginning to slide. At $t = 2$ h, impact and impact and sliding groups were impacted; immediately following impact, explants in group impact and sliding were mounted onto the tribometer and allowed to stress relax for 1 h before beginning to slide. After group impact and sliding completed sliding, $t = 4$ h, all explants in each of the four treatment groups were axially bisected into hemicylinders, with each hemicylinder being stained for either cell viability, mitochondrial polarization, or caspase activity. Imaging of explants began at $t = 7$ h, after 3 h post-injury of the impact and sliding group.

2.5 | Fluorescent staining and imaging

Cylindrical samples were axially bisected into hemicylinders and stained either for 30 min with 1 μl/ml Calcein AM and 1 μl/ml ethidium homodimer (Thermo Fisher Scientific), 30 min with CellEvent Caspase-3/7 Green (Thermo Fisher Scientific) following manufacturer instructions, or MitoTracker Green (200 nM; Thermo Fisher Scientific) for 20 min followed by addition of tetramethylrhodamine methyl ester perchlorate (10 nM; Thermo Fisher Scientific) for 20 min. After staining, all explants were rinsed in DPBS for 5 min. Cartilage explants were imaged on a Zeiss LSM880 confocal/multiphoton inverted microscope to determine the cellular responses to rapid impact injury, repeated frictional shear, or the combination of both.

Confocal images were captured and imported into ImageJ to create a composite image (550 μm wide × 725 μm depth). Depth-dependent cellular responses were quantified using Fiji (NIH) a custom MATLAB program (MathWorks, Inc.).[30,31,43] Global tissue responses were reported as percentage cell death (100 × total red cells/total red and green cells), percent cells with depolarized MT (100 × total green cells/total cells colocalizing red and green), and number of caspase-positive cells normalized to the area of the composite image, 0.39875 mm^2. Depth-dependent results were calculated by segmenting each image into 18 depth-dependent bins (~40 μm depth × 550 μm wide) with all bins using the same image analysis outcomes. The number of caspase-positive cells were normalized to the area of the bin, 0.022153 mm^2.

2.6 | Statistical analysis

Two-way ANOVAs were performed to compare the effects of impact, sliding, and performing both in succession. Differences were considered statistically significant at $p \leq .05$, for both global tissue and depth-dependent results. Comparisons between groups were performed using Tukey's HSD method. Depth-dependent results were fit to a stretched exponential curve where the results of each stain were plotted as a function of x, distance away from the cartilage articular surface, given by

$$y(x) = P + (Y_o - P)e^{-(x/\lambda)^d},$$

where Y_o represents the magnitude of damage at the articular surface, P represents the magnitude of damage in the middle zone of the tissue, λ represents the depth from the articular surface at the midpoint of the transition from the highest to lowest magnitude in the model, and d is a fitting parameter controlling the slope of the transition.

Parameters for cell death and MT depolarization were subjected to the constraints: 100% ≥ Y_o and $P \geq 0\%$, $\lambda \geq 50$, and $d \geq 0$; while parameters from number of apoptotic cells were subjected to the constraints: highest number of apoptotic cells in an individual bin ≥ Y_o and $P \geq 0$, $\lambda \geq 50$, and $d \geq 0$. These constraints were placed on the model to constrict values to non-zero results between 0% and 100%, and to ensure that λ was not smaller the bin size used to track depth dependent results. Goodness of fit between the data and the model was characterized by the R^2 values attained by plotting the data against the values obtained through the model. Two-way ANOVAs and Tukey's HSD tests were then used to compare the values of P, Y_o, and λ between all groups for each of the three stains used. Nonlinear modeling and statistical analyses and were performed using GraphPad Prism 7 software.

3 | RESULTS

3.1 | Experiments

Our study entailed a detailed comparison of cartilage damage as a function of mechanical loading (Figure 1). To conduct this study, we harvested cartilage explants and subjected them to one of four loading conditions as outlined by the timelines in Figure 1: control, slid, impacted, or impacted and slid. Following these protocols, tissues were bisected and stained to assess cell death, apoptosis, and MT depolarization using procedures described in the Methods section.

3.2 | Confocal images

Confocal microscopy of the tissue samples (Figure 2) indicated clear spatial patterns of tissue response with magnitude of damage increasing in order of least to greatest for the control (left column), slid (left-middle column), impact (right-middle column), and impacted and slid (right column) conditions. We observed that cell death (red) was concentrated at the surface and penetrated deeper into the tissue for the impacted and impacted and slid conditions. We also observed that the deeper regions of the tissue contained a combination of live and dead cells in the impacted and slid condition. Similarly, we observe that caspase activity (green in

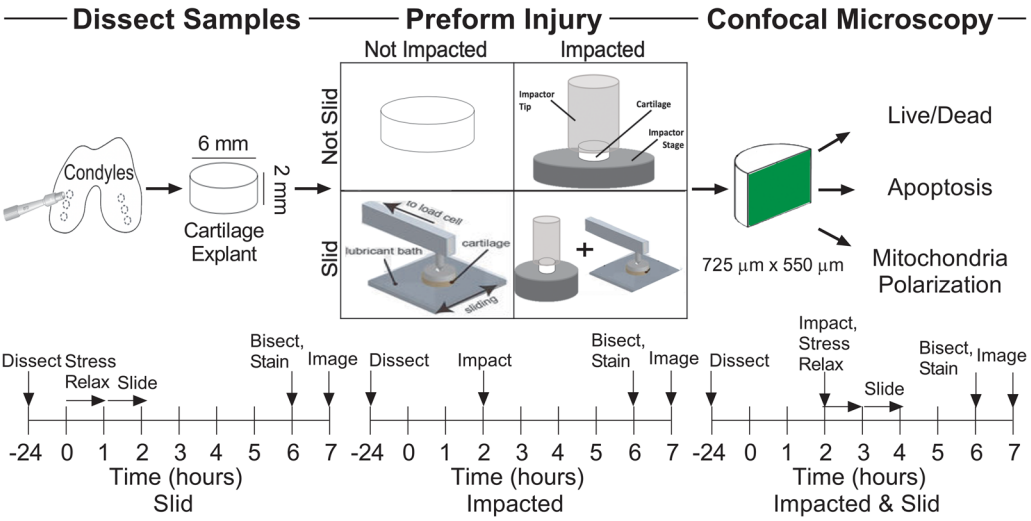

FIGURE 1 Experimental design and methods [Color figure can be viewed at wileyonlinelibrary.com]

Figure 2B), often a precursor to apoptosis, increases both in magnitude and depth as we vary the condition from control to impacted and slid (note that the white dots are image artifacts that arise from image tiling). Finally, we find that mitochondrial depolarization (green in Figure 2C) also increased in magnitude and depth as we varied the conditions from control to impacted and slid. Here too, we observed a greater mixing of polarized and depolarized mitochondrial populations for the impacted and impacted and slid conditions. We used a newly developed algorithm to quantify these observed spatial patterns as described in Section 2, and report these measurements below.

3.3 | Global tissue analysis

Measurements of cell death, caspase activity, and mitochondrial polarization averaged over the entire imaging region showed clear progression of damage as the condition varied from control, to slid, impacted, and impacted and slid. However, we observed a high degree of sample to sample variations due to differences in extent of localization of damage between conditions. Despite these variations, clear patterns in cell damage were noted based on type of injury. Cell death measurements showed the impacted and slid condition reached the highest magnitude of damage at 63.0% cell death, with impacted at a similar level of 51.9% ($p = .0802$). Slid induced the lowest amount of cell death of all loading modalities at 26.5%, however was still greater than that of the control group ($p = .0006$). Caspase activity followed a similar trend as cell death with impacted and slid achieving the greatest response at 747 apoptotic cells/mm^2, with impacted at a similar magnitude of 616 apoptotic cells/mm^2 ($p > .05$). However, the response of slid, 525 apoptotic cells/mm^2, was similar to that of controls and the other loading modalities ($p > .05$). Finally, assessments of MT depolarization showed that impacted and slid led to the highest magnitude of response at 69.6%. This result was higher than that of impacted at 44.8% ($p = .0008$) or slid at 18.1% ($p < .0001$). Impacted and slid led to an increase of MT depolarization greater than impacted or slid (Figure 3C) ($p = .016$ for interaction via two-way ANOVA). The degree of variation in the measurements averaged over the entire region of interest suggests that depth dependent data may be more appropriate for statistically distinguishing magnitude of damage across the different loading conditions.

3.4 | Depth-dependent tissue analysis

Indeed, we find that reporting the outcomes as a function of depth by segmenting the region of interest into bins ~40 μm in depth enables us to further distinguish the outcomes due to the different loading conditions and observe clear differences in surface and middle zone responses (Figure 4A-C). Again, we detect a similar order of tissue response as seen in our global analysis with magnitude of damage increasing in order of least to greatest: control (grey circle), slid (red circle), impacted (red x), and impacted and slid (red circle with x). This hierarchy of tissue response was observed in both the cartilage surface and middle zones. Cell death, apoptosis, and MT polarization showed minimal damage in the control samples beyond a depth of 100 μm. However, all loading conditions produced greater cell death compared to controls within the surface zone ($p < .0264$), while impacted and impacted and slid showed greater cell death than controls throughout the middle zone as well ($p < .0473$). Apoptosis measurements revealed slid and impacted induced greater response compared to controls within the surface zone up to depths of 260 μm, while impacted and slid induced greater damage up to depths of 540 μm. Finally, MT depolarization in the slid group was minimal past 100 μm and was only greater than controls up to depths of 60 μm (Figure 4C). Impacted and impacted and slid caused MT depolarization greater than controls

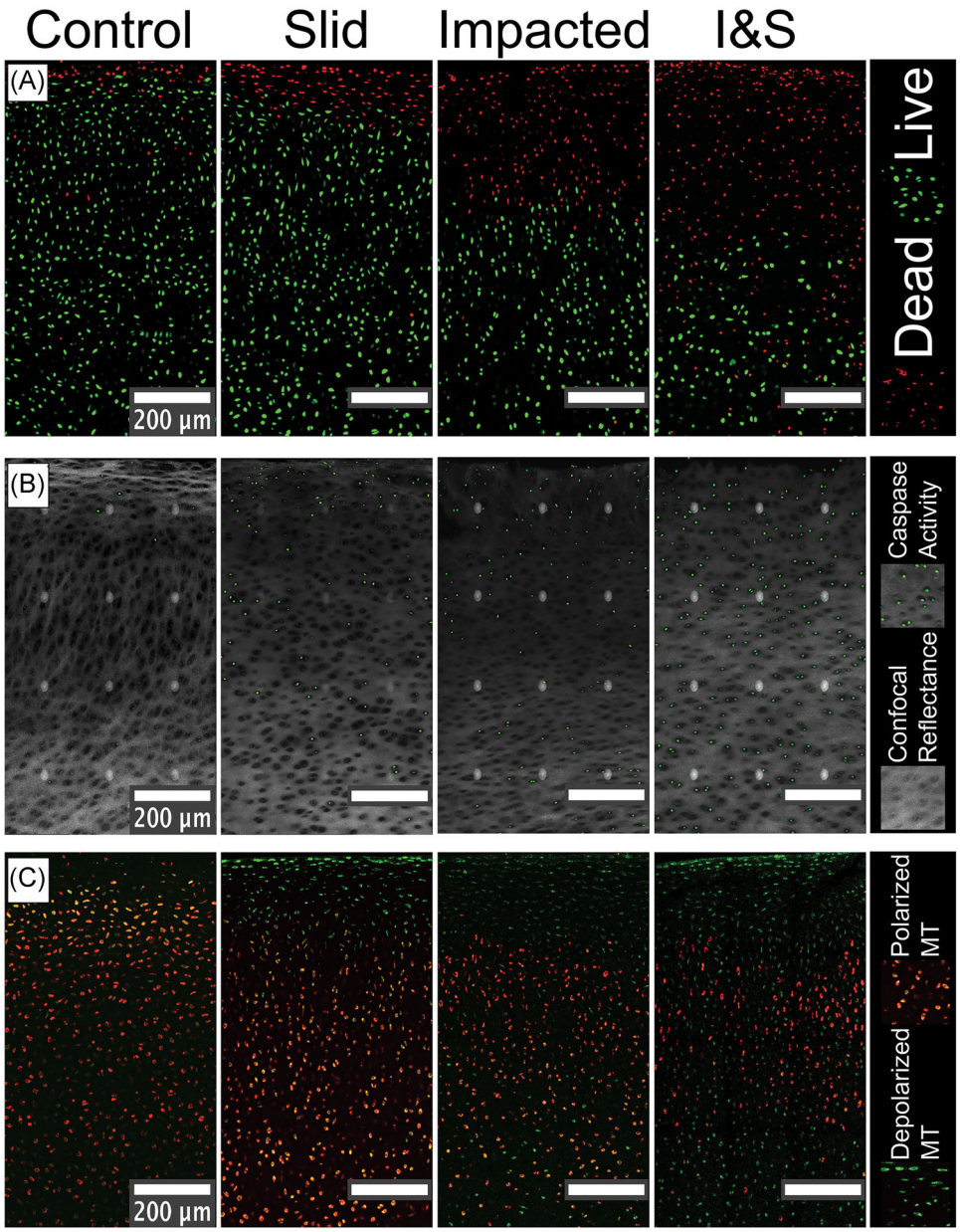

FIGURE 2 Confocal images of all groups [Color figure can be viewed at wileyonlinelibrary.com]

throughout the surface zone ($p < .0027$). However, impacted and slid propagated MT depolarization greater than controls throughout the entire middle zone ($p < .0001$)

To quantify and compare the degree of damage reached at the articular surface and middle zone across conditions, we use nonlinear modeling via fits (Section 2) to a stretched exponential plus an offset: $y(x) = P + (Y_0\text{-}P) * e^{-(x/y)^d}$ (solid curves in Figure 4). In this model, Y_o represents the magnitude of damage at the articular surface, P represents the magnitude of damage in the middle zone of the tissue, λ represents the depth from the articular surface at the mid-point of the transition from the highest to lowest magnitude in the model, and d is a fitting parameter controlling the slope of the transition. The detailed results for the fits are reported in Table 1. The range of goodness of fit for all models ranged between 0.8915 and 0.9896. We report the dependence of the parameters Y_o, P, and λ on the testing condition in Figure 5.

For all injury groups, the magnitude of damage at the articular surface, Y_o, was high and reached a minimum of 88.6% cell death, 1055 apoptotic cells/mm^2, and 92.8% MT depolarization. The magnitude of damage was not significantly different between slid, impacted, and impacted and slid at the articular surface (Figure 5A,D,G). Cell death and apoptosis at the surface were similar between injured and control samples ($p > .05$), while MT depolarization at the surface was lower in controls than injured groups ($p < .012$).

The magnitude of damage reached at the middle zone, P, was minimally affected in the slid condition and was only higher than controls in cell death ($p = .025$) (Figure 5B). For apoptosis, none of the groups were different from one another ($p > .05$), however

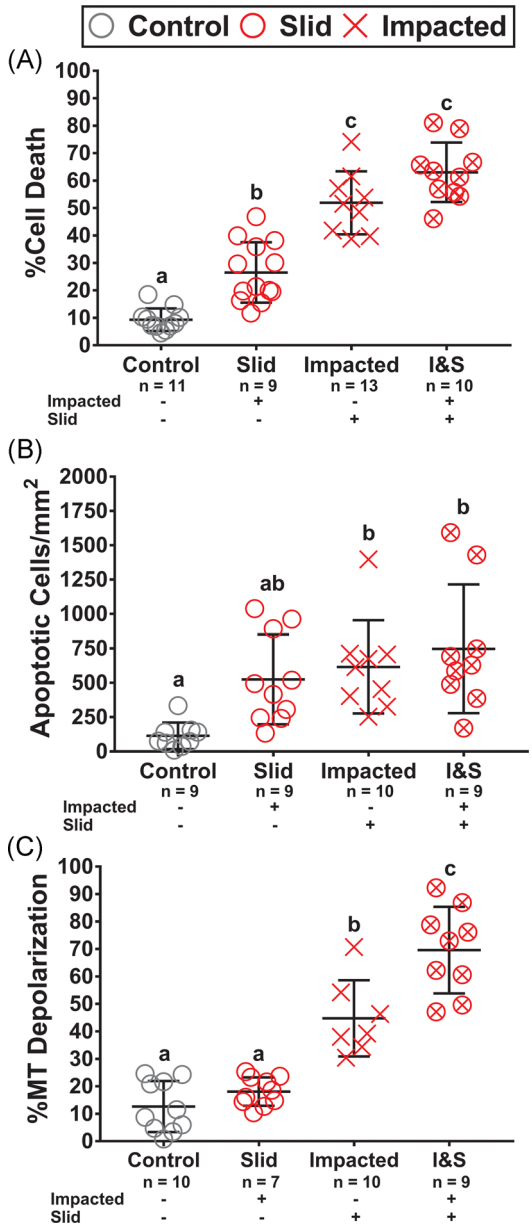

FIGURE 3 Global tissue analysis results [Color figure can be viewed at wileyonlinelibrary.com]

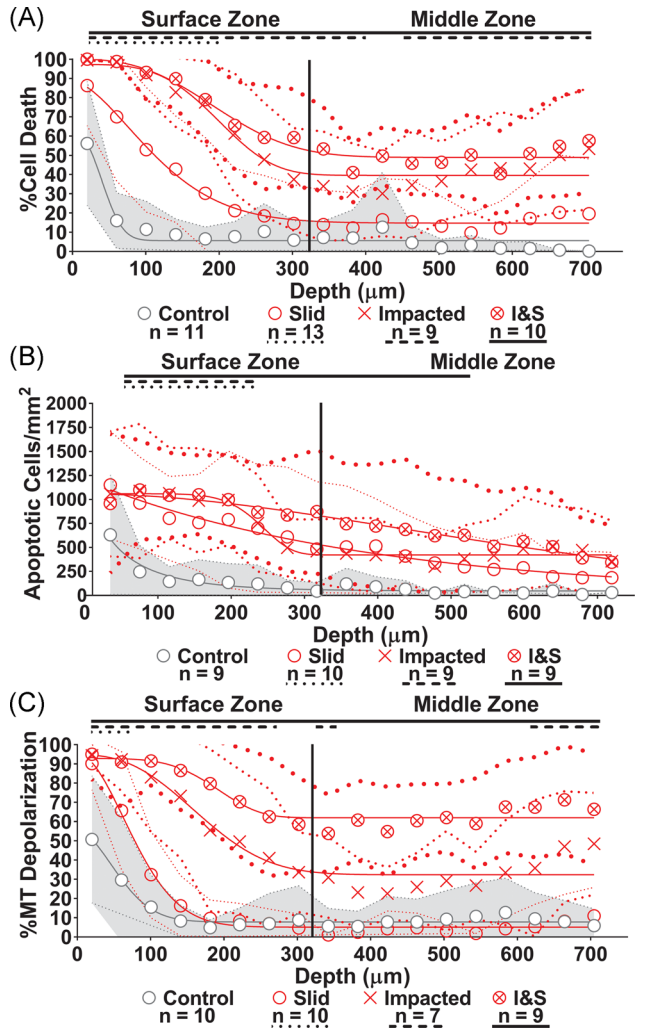

FIGURE 4 Depth-dependent analysis results with nonlinear curve fit [Color figure can be viewed at wileyonlinelibrary.com]

impacted had the highest damage with 422 apoptotic cells/mm^2 present at the middle zone (Figure 5E). For cell death and MT depolarization, impacted and slid had the highest levels of damage at the middle zone, followed by impacted. Impacted and slid caused 48.9% cell death and 62.0% MT depolarization at the middle zone while impacted caused 39.6% cell death and 32.3% MT depolarization and was statistically higher in both cases ($p < .0119$) (Figure 5B,H). The combination of impacting and sliding was again additive for cell death and greater than additive for MT depolarization ($p < .0001$ for interaction via two-way ANOVA).

The stretched exponential model revealed that for all outcome measures, the mid-point of damage, λ, of impacted and slid occurred deeper into the tissue compared to either slid or impacted ($p < .05$). The mid-point of impacted and slid and was not reached until a minimum depth of 205 μm (Figure 5I) and a maximum depth of 665 μm (Figure 5F). For cell death and MT depolarization the mid-point of impacted and slid was similar to impacted ($p > .05$) and higher than the midpoint of slid ($p = .005$) (Figures 5C,I). Impacted groups having the deepest midpoints of damage indicates that impact is most responsible for propagating cell death and MT depolarization into deeper regions of cartilage. For apoptosis, the midpoint of slid damage, occurred at a depth of 389 μm, while the midpoint for impacted occurred at a depth of 235 μm ($p > .05$) (Figure 5F). While not significantly different, slid groups having deeper midpoints for apoptosis may indicate that sliding is most responsible for propagating damage into deeper regions of the cartilage, rather than impact. Overall, the hierarchy of greatest cause of cellular damage was impacted and slid, followed by impacted, followed by sliding. This model showed of the three outcome measures, MT depolarization was observed most frequently following injury. MT depolarization reached the highest amount of response globally and throughout the depth of the tissue. Following MT depolarization,

TABLE 1 Stretched exponential model results

$y(x) = (Y_0\text{-}P) * e^{-(x/\lambda)^d} + P$										
Stain/group	***N***	Y_o	***SEM***	***P***	***SEM***	λ	***SEM***	***d***	**SEM**	R^2
Live/dead										
Control	11	61.7	53.3	5.64	1.04	50.0	41.2	2.44	7.38	0.9141
Slid	9	88.6	8.6	14.74	2.05	134.8	16.8	1.64	0.47	0.9844
Impacted	13	97.3	5.3	39.57	2.51	218.6	16.6	3.74	1.44	0.9353
I&S	10	100.0	4.7	48.92	2.13	225.3	19.0	2.74	0.87	0.9529
Apoptosis										
Control	9	928.9	645.2	46.48	24.69	50.0	53.7	0.79	0.61	0.9321
Slid	9	1161.1	235.7	0.00	390.77	389.5	232.8	0.99	0.51	0.9753
Impacted	10	1059.0	76.1	421.74	43.67	235.8	18.8	7.10	5.09	0.9689
I&S	9	1054.8	137.1	45.29	2261.70	665.0	1379.7	1.77	2.12	0.9609
MT Depolarization										
Control	10	55.0	10.7	7.81	1.34	70.3	14.8	1.85	1.10	0.9689
Slid	7	95.4	6.0	5.10	1.11	94.7	6.2	1.88	0.33	0.9896
Impacted	10	94.7	8.3	32.33	3.17	191.8	23.6	2.57	1.13	0.9176
I&S	9	92.8	4.9	61.96	2.26	205.1	24.9	4.46	3.28	0.8915

Note: Results from fitting experimental data to stretched exponential model. Live/dead and MT depolarization are reported as percentages while apoptosis is reported as # of cells/mm^2. *SEM* represents standard error of the mean and R^2 represents the correlation between the model values and experimental values.

cell death was next most affected while apoptosis showed the least amount of response from mechanical injury.

4 | DISCUSSION

In this paper, we developed a new and robust ex vivo model of PTOA to more closely mimic the mechanical environment in cartilage after articular injury. We've also developed a statistical method able to characterize results by evaluating degree of injury in a global and depth-dependent manner. Using this model, we observed the combined effects of two types of loading experienced in joints during and after trauma, namely rapid compression and cyclic shear. Our results show that while both impact injury and sliding motion affect the health of chondrocytes, sliding previously impacted tissue led to aggravated chondrocyte damage throughout the depth of the cartilage. Assessments of cell death and apoptosis, looking at the global tissue and spatially through the depth, show that combining both loading modalities had an additive effect. Traumatic injury seems to impair the protective qualities of the surface region and prime chondrocytes for further damage that is propagated by the shear loading caused by sliding motion. The results of this study would imply that those who receive injuries associated with PTOA development, such as anterior cruciate ligament rupture and meniscus tears, would be susceptible to exacerbating their injury by articulating injured joints shortly after initial injury.[4]

Our results showed that damage is primarily concentrated at the articular surface and indicates that impacting, sliding, or both will cause the cartilage surface to be most affected. Damage generated by injury was seen to drop to half its maximum at about halfway through the surface zone. The severe decline of damage at the surface zone shows that the surface acts as a protective layer to limit damage propagation deeper into the tissue.[30,31] Previous studies have shown the surface acts as the primary shear energy dissipating region with damage to this region exacerbating the effect of shear stress elsewhere in the tissue, which is consistent with the results of this study.[44-46] The protective nature of cartilage could be due to its inhomogeneous nature where the superficial layer is more compliant than the bulk, which results in the strain, and therefore the majority of cellular damage, being concentrated at the surface.[46,47] Next, the cellular damage caused by sliding motion is consistent with previous studies showing that the shear strain produced, at physiologic sliding speeds, similar levels of chondrocyte death at the superficial layer.[30] Minor superficial cracking without fibrillation was observed at the cartilage surface, which may be responsible for the increased damage in cartilage that was impacted before sliding is due to the integrity of the superficial layer being compromised, making it resemble cartilage samples in previous studies where the surface is removed before impact.[31,45] This shows the need of an alternative shear energy dissipation mechanism once the surface becomes compromised. Lubrication of the cartilage sliding surfaces has been shown to assist in this function with alteration to the lubricant's lubricating properties being capable of mitigating or agitating cell death.[48] Our results show that the heterogeneity of cartilage result in significant differences in the strains experienced throughout the tissue, which affects the patterns of cellular damage that occurs as a consequence to injury.

The combination of impacting and sliding caused a synergistic increase of MT depolarization, particularly past the surface zone in deeper regions of the tissue. Synergistic increase in MT depolarization may indicate that the MT are highly sensitive to

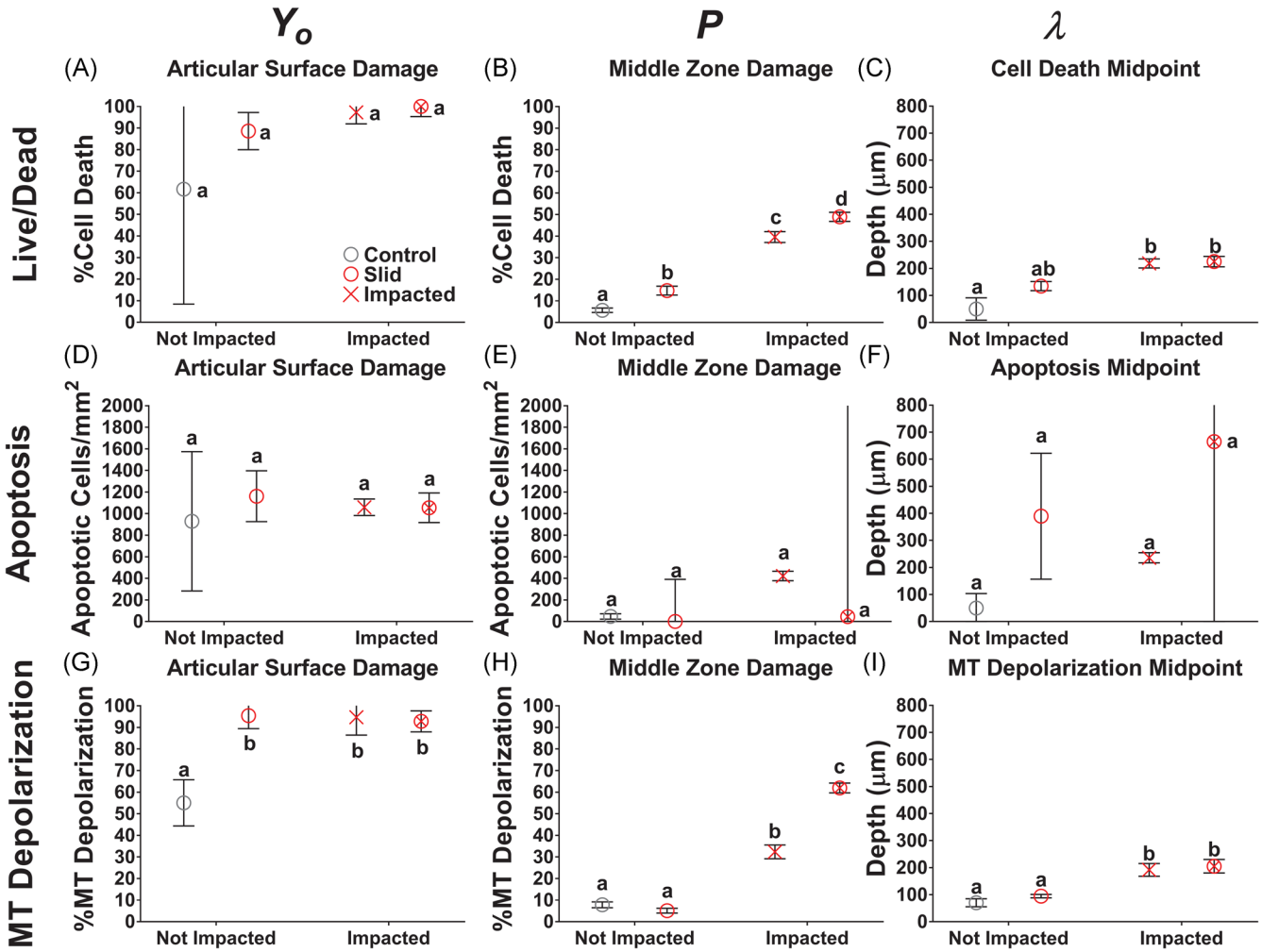

FIGURE 5 Comparison of parameters from nonlinear model [Color figure can be viewed at wileyonlinelibrary.com]

mechanical injury. Recent evidence suggests that MT dysfunction is central to chondrocyte's response to trauma and is related to local tissue mechanics; increased friction leads to in increased tissue strain and results in increased MT depolarization.[20,30] A possible mechanism for this synergy is that impact injury damages cartilage such that further loading causes higher strains within the injured joint. In particular, it has been demonstrated that impact injury causes cracking of the cartilage matrix, which in turn may cause a positive feedback loop of abnormal stresses around the crack that further propagates it.[49,50] Higher strains could be the result of a loss in cartilage stiffness due to the presence of microcracks present throughout the tissue that grow in size as the tissue is further articulated. While temporary joint immobilization may provide limited benefits, it is possible that delayed sliding of cartilage tissue with damaged collagen networks will induce similar levels of cell damage as immediate sliding due to the limited capability of collagen repair by chondrocytes. Cartilage self-repair occurs to a limited degree with fibrocartilage,[51] which possess inferior mechanical properties to normal cartilage tissue, meaning once the extracellular matrix becomes compromised, the cartilage will experience increased strains and is therefore predisposed to exacerbated cellular damage.

There are several limitations to consider when interpreting these data such as using neonatal cartilage tissue, which may be more susceptible to damage compared to mature tissue.[52,53] Due to cartilage becoming more stiff with age, particularly within the deep zone, use of neonatal cartilage may have resulted in cartilage damage that is more pronounced than would be seen in mature tissue.[54] Neonatal cartilage was selected for use due to higher levels of chondrocytes present within the cartilage matrix, its consistency and reproducibility as a tissue source.[55,56] Many groups have also used neonatal cartilage to study PTOA in particular, which further validates its use as a tissue source for this study.[57] Also, unlike other forms of OA, PTOA generally develops in younger populations that are more active, which may make the use of neonatal cartilage as a tissue source appropriate when studying PTOA.[58] Furthermore, impacting cartilage explants using a flat tip that covers the surface, without subchondral bone underneath, affects the boundary conditions of the impact and may change the thresholds for damage from what would be experienced in vivo. The loading profile used, static

compression at 15% strain for 1 h, was also limited in its physiologic relevancy due to joint motion being able to produce larger and less stable strains on cartilage. In addition, subjecting cartilage explants to the combined loading of sliding and a constant 15% compression may contribute to the increased cellular damage observed in this study. Also, while using polished glass as the counterface during the sliding process may mimic the joint environment, further studies may aim to use an in vivo model where cartilage on cartilage articulation is present. Next, use of Calcein AM and ethidium homodimer results in indirect measurements of cell death via cell membrane permeability whereas techniques such as TUNEL staining would directly measure cell death occurring via apoptosis.[59] As such, cell death data presented above may not truly be cell death in the absence of TUNEL staining and future work may seek to add TUNEL staining to the staining protocol. Furthermore, the difficulty of reproducing environmental conditions that result in physiologic MT oxygen consumption, membrane potential, or respiratory chain complex activity[12,15] ex vivo is further indication that in vivo studies would be beneficial.

In summary, this study demonstrated, both globally and in a depth-dependent manner, that mechanical injury followed by repetitive sliding exacerbated cellular damage compared to either injury or sliding alone. A possible mechanism for reducing the level of MT depolarization and cell death would be to decrease the shear load experienced at the articular surface through viscosupplementation of the lubricating fluid, which is supported by results from previous studies.[47,48,60] Our results reveal a concentration of damage at the cartilage articular surface, which persisted at a high magnitude throughout the middle zone in cartilage that was impacted and slid. At the middle zone, the MT in particular saw a high degree of damage, leaving a sizable population of viable chondrocytes with MT depolarization. The population of cells with MT depolarization represents a possible mechanism by which damage spreads to other areas of the tissue and joint. As such, viable cells experiencing MT depolarization represents a potential target for treatment through therapeutics that are able to specifically target the MT to restore its bioenergetic function.[21,61,62]

ACKNOWLEDGMENTS

The study was supported by the National Institutes of Health (NYSTEM CO29155, NIH S10OD018516, NIH-NIAMS 1R03AR075929-01, NIH-NIAMS 5K08AR068470-02), NSF (NSF CMMI-1536463, NSF DMR-1807602), Harry M. Zweig Memorial Fund for Equine Research, and Alfred P. Sloan Foundation.

CONFLICT OF INTERESTS

Dr. Bonassar is a cofounder of and holds equity in 3DBio Corp and is a consultant for Fidia Farmaceutici, SpA.

AUTHOR CONTRIBUTIONS

Steven Ayala, Michelle L. Delco, Lisa A. Fortier, Itai Cohen, and Lawrence J. Bonassar contributed to experimental design, data analysis, manuscript writing, and manuscript editing. Steven Ayala and Michelle L. Delco performed all experiments.

ORCID

Steven Ayala http://orcid.org/0000-0003-2372-5680
Michelle L. Delco https://orcid.org/0000-0003-0973-2075

REFERENCES

1. Brown TD, Johnston RC, Saltzman CL, et al. Posttraumatic osteoarthritis: A first estimate of incidence, prevalence, and burden of disease. *J Orthop Trauma*. 2006;20(10):739-744.
2. Thomas AC, Hubbard-Turner T, Wikstrom EA, Palmieri-Smith RM. Epidemiology of posttraumatic osteoarthritis. *J Athl Train*. 2017;52(6):491-496.
3. Dell'Isola A, Allan R, Smith SL, et al. Identification of clinical phenotypes in knee osteoarthritis: a systematic review of the literature. *BMC Musculoskelet Disord*. 2016;17(1):1-12.
4. Carbone A, Rodeo S. Review of current understanding of posttraumatic osteoarthritis resulting from sports injuries. *J Orthop Res*. 2017;35(3):397-405.
5. Aspden RM, Jeffrey JE, Burgin LV. Letter to the editor. *Osteoarthr. Cartil*. 2002;10(7):588-589.
6. Murphy L, Schwartz TA, Helmick CG, et al. Lifetime risk of symptomatic knee osteoarthritis. *Arthritis Care Res*. 2008;59(9):1207-1213.
7. Rodeo S, Joseph AB, Lotz M. Special Issue: Injury and post-traumatic osteoarthritis. *J Orthop Res*. 2017;35(3):395-396.
8. Whittaker JL, Roos EM. A pragmatic approach to prevent post-traumatic osteoarthritis after sport or exercise-related joint injury. *Best Pract Res Clin Rheumatol*. 2019;33(1):158-171. https://doi.org/10.1016/j.berh.2019.02.008
9. Whittaker JL, Woodhouse LJ, Nettel-Aguirre A, Emery CA. Outcomes associated with early post-traumatic osteoarthritis and other negative health consequences 3-10 years following knee joint injury in youth sport. *Osteoarthr Cartil* 2015;23(7):1122-1129. Available from https://doi.org/10.1016/j.joca.2015.02.021
10. Lieberthal J, Sambamurthy N, Scanzello CR. Inflammation in joint injury and post-traumatic osteoarthritis. *Osteoarthr Cartil* 2015;23(11):1825-1834. Available from https://doi.org/10.1016/j.joca.2015.08.015
11. Anderson DD, Chubinskaya S, Guilak F, et al. Post-traumatic osteoarthritis: Improved understanding and opportunities for early intervention. *J Orthop Res*. 2011;29(6):802-809.
12. Delco ML, Bonnevie ED, Bonassar LJ, Fortier LA. Mitochondrial dysfunction is an acute response of articular chondrocytes to mechanical injury. *J Orthop Res*. 2018;36(2):739-750.
13. Delco ML, Bonnevie ED, Szeto HS, et al. Mitoprotective therapy preserves chondrocyte viability and prevents cartilage degeneration in an ex vivo model of posttraumatic osteoarthritis. *J Orthop Res*. 2018.
14. Lõpez De Figueroa P, Lotz MK, Blanco FJ, Caramés B. Autophagy activation and protection from mitochondrial dysfunction in human chondrocytes. *Arthritis Rheumatol*. 2015;67(4):966-976.
15. Liu H, Li Z, Cao Y, et al. Effect of chondrocyte mitochondrial dysfunction on cartilage degeneration: A possible pathway for osteoarthritis pathology at the subcellular level. *Mol Med Rep*. 2019;20(4):3308-3316.
16. Maneiro E, Martín MA, De Andres MC, et al. Mitochondrial respiratory activity is altered in osteoarthritic human articular chondrocytes. *Arthritis Rheum*. 2003;48(3):700-708.
17. Gavriilidis C, Miwa S, Von Zglinicki T, et al. Mitochondrial dysfunction in osteoarthritis is associated with down-regulation of superoxide dismutase 2. *Arthritis Rheum*. 2013;65(2):378-387.

18. Gerencser AA, Chinopoulos C, Birket MJ, et al. Quantitative measurement of mitochondrial membrane potential in cultured cells: calcium-induced de- and hyperpolarization of neuronal mitochondria. *J Physiol*. 2012;590(12):2845-2871.
19. Zorova LD, Popkov VA, Plotnikov EY, et al. Mitochondrial membrane potential. *Anal Biochem*. 2018;552:50-59.
20. Bartell LR, Fortier LA, Bonassar LJ, et al. Mitoprotective therapy prevents rapid, strain-dependent mitochondrial dysfunction after articular cartilage injury. *J Orthop Res*. 2019;38(6):1257-1267. https://doi.org/10.1002/jor.24567
21. Szeto HH, Liu S. Cardiolipin-targeted peptides rejuvenate mitochondrial function, remodel mitochondria, and promote tissue regeneration during aging. *Arch Biochem Biophys*. 2018;660(October):137-148.
22. Sweeney EA, Howell DR, James DA, et al. Returning to Sport after Gymnastics Injuries. *Curr Sports Med Rep*. 2018;17(11):376-390.
23. Hinman RS, Heywood SE, Day AR. Aquatic physical therapy for hip and knee osteoarthritis: results of a single-blind randomized controlled trial. *Phys Ther*. 2007;87(1):32-43.
24. Deyle GD, Henderson NE, Matekel RL, Ryder MG, Garber MB, SCA. Effectiveness of manual physical therapy and exercise in osteoarthritis of the knee. A randomized, controlled trial. *Ann Intern Med*. 2000;132(3):173-181.
25. Mutsuzaki H, Nakajima H, Sakane M. Extension of knee immobilization delays recovery of histological damages in the anterior cruciate ligament insertion and articular cartilage in rabbits. *J Phys Ther Sci*. 2018;30(1):140-144.
26. Mutsuzaki H, Nakajima H, Wadano Y, et al. Influence of knee immobilization on chondrocyte apoptosis and histological features of the anterior cruciate ligament insertion and articular cartilage in rabbits. *Int J Mol Sci*. 2017;18(2):253.
27. Tyler TF, Lung JY. Rehabilitation following osteochondral injury to the knee. *Curr Rev Musculoskelet Med*. 2012;5(1):72-81.
28. Pauly HM, Larson BE, Coatney GA, et al. Assessment of cortical and trabecular bone changes in two models of post-traumatic osteoarthritis. *J Orthop Res*. 2015;33(12):1835-1845.
29. Bonnevie ED, Delco ML, Fortier LA, et al. Characterization of tissue response to impact loads delivered using a hand-held instrument for studying articular cartilage injury. *Cartilage*. 2015;6(4):226-232.
30. Bonnevie ED, Delco ML, Bartell LR, et al. Microscale frictional strains determine chondrocyte fate in loaded cartilage. *J Biomech*. 2018;74:72-78.
31. Bartell LR, Fortier LA, Bonassar LJ, Cohen I. Measuring microscale strain fields in articular cartilage during rapid impact reveals thresholds for chondrocyte death and a protective role for the superficial layer. *J Biomech*. 2015;48(12):3440-3446. https://doi.org/10.1016/j.jbiomech.2015.05.035
32. Bonnevie ED, Delco ML, Galesso D, et al. Sub-critical impact inhibits the lubricating mechanisms of articular cartilage. *J Biomech*. 2017;53:64-70.
33. Steineman BD, Laprade RF, Santangelo KS, et al. Early osteoarthritis after untreated anterior meniscal root tears: An in vivo animal study. *Orthop J Sport Med*. 2017;5(4):1-14.
34. Exler Y. Patella fracture: review of the literature and five case presentations. *J Orthop Sports Phys Ther*. 1991;13(4):177-183.
35. Boeth H, Duda GN, Heller MO, et al. Anterior cruciate ligament-deficient patients with passive knee joint laxity have a decreased range of anterior-posterior motion during active movements. *Am J Sports Med*. 2013;41(5):1051-1057.
36. Alexander PG, Song Y, Taboas JM, et al. Development of a spring-loaded impact device to deliver injurious mechanical impacts to the articular cartilage surface. *Cartilage*. 2013;4(1):52-62.
37. Noyes FR, Grood ES. The strength of the anterior cruciate ligament in humans and rhesus monkeys: age related and species related changes. *J Bone Jt Surg Ser A*. 1976;58(8):1074-1082.
38. D'Lima DD, Hashimoto S, Chen PC, et al. Human chondrocyte apoptosis in response to mechanical injury. *Osteoarthr Cartil* 2001;9(8):712-719.
39. Gleghorn JP, Jones ARC, Flannery CR, Bonassar LJ. Boundary mode lubrication of articular cartilage by recombinant human lubricin. *J Orthop Res*. 2009;27(6):771-777.
40. Bonnevie ED, Galesso D, Secchieri C, et al. Elastoviscous transitions of articular cartilage reveal a mechanism of synergy between lubricin and hyaluronic acid. *PLOS One*. 2015;10(11):1-15.
41. Buckley MR, Bergou AJ, Fouchard J, et al. High-resolution spatial mapping of shear properties in cartilage. *J Biomech*. 2010;43(4):796-800. https://doi.org/10.1016/j.jbiomech.2009.10.012
42. Gleghorn JP, Bonassar LJ. Lubrication mode analysis of articular cartilage using Stribeck surfaces. *J Biomech*. 2008;41(9):1910-1918.
43. Schindelin J, Arganda-Carreras I, Frise E, et al. Fiji: an open-source platform for biological-image analysis. *Nat Methods*. 2012;9:676-682.
44. Kaleem B, Maier F, Drissi H, Pierce DM. Low-energy impact of human cartilage: predictors for microcracking the network of collagen. *Osteoarthr Cartil*. 2017;25(4):544-553. https://doi.org/10.1016/j.joca.2016.11.009
45. Bartell LR, Xu MC, Bonassar LJ, Cohen I. Local and global measurements show that damage initiation in articular cartilage is inhibited by the surface layer and has significant rate dependence. *J Biomech*. 2018;72:63-70.
46. Buckley MR, Bonassar LJ, Cohen I. Localization of viscous behavior and shear energy dissipation in articular cartilage under dynamic shear loading. *J Biomech Eng*. 2013;135(3):1-9.
47. Wong BL, Bae WC, Chun J, et al. Biomechanics of cartilage articulation: Effects of lubrication and degeneration on shear deformation. *Arthritis Rheum*. 2008;58(7):2065-2074.
48. Waller KA, Zhang LX, Elsaid KA, et al. Role of lubricin and boundary lubrication in the prevention of chondrocyte apoptosis. *Proc Natl Acad Sci USA*. 2013;110(15):5852-5857.
49. Zhong D, Zhang M, Yu J, Luo ZP. Local tensile stress in the development of posttraumatic osteoarthritis. *BioMed Res Int*. 2018;2018.
50. Sadeghi H, Lawless BM, Espino DM, Shepherd DET. Effect of frequency on crack growth in articular cartilage. *J Mech Behav Biomed Mater*. 2018;77(August):40-46.
51. Wang KH, Wan R, Chiu LH, et al. Effects of collagen matrix and bioreactor cultivation on cartilage regeneration of a full-thickness critical-size knee joint cartilage defects with subchondral bone damage in a rabbit model. *PLOS One*. 2018;13(6):1-15.
52. Kurz B, Lemke A, Kehn M, et al. Influence of tissue maturation and antioxidants on the apoptotic response of articular cartilage after injurious compression. *Arthritis Rheum*. 2004;50(1):123-130.
53. Levin AS, Chen CTC, Torzilli PA. Effect of tissue maturity on cell viability in load-injured articular cartilage explants. *Osteoarthr Cartil*. 2005;13(6):488-496.
54. Gannon AR, Nagel T, Bell AP, et al. Postnatal changes to the mechanical properties of articular cartilage are driven by the evolution of its collagen network. *Eur Cells Mater*. 2015;29:105-123.
55. Mauch KA, Katwal AB, Seyedin M. The potential of human allogeneic juvenile chondrocytes for restoration of articular cartilage. *Am J Sport Med*. 2013;38(7):1324-1333.
56. Adkisson HD, Milliman C, Zhang X, et al. Immune evasion by neocartilage-derived chondrocytes: implications for biologic repair of joint articular cartilage. *Stem Cell Res*. 2010;4(1):57-68. https://doi.org/10.1016/j.scr.2009.09.004
57. Torre OM, Das R, Berenblum RE, et al. Neonatal mouse intervertebral discs heal with restored function following herniation injury. *FASEB J*. 2018;32(9):4753-4762.
58. Buckwalter JA, Anderson DD, Brown TD, et al. The roles of mechanical stresses in the pathogenesis of osteoarthritis:

implications for treatment of joint injuries. *Cartilage*. 2013;4(4):286-294.
59. Ziegler U, Groscurth P. Morphological features of cell death. *News Physiol Sci*. 2004;19(3):124-128.
60. Flannery CR, Zollner R, Corcoran C, et al. Prevention of cartilage degeneration in a rat model of osteoarthritis by intraarticular treatment with recombinant lubricin. *Arthritis Rheum*. 2009;60(3):840-847.
61. Szeto HH. First-in-class cardiolipin-protective compound as a therapeutic agent to restore mitochondrial bioenergetics. *Br J Pharmacol*. 2014;171(8):2029-2050.
62. Zhao K, Zhao GM, Wu D, et al. Cell-permeable peptide antioxidants targeted to inner mitochondrial membrane inhibit mitochondrial swelling, oxidative cell death, and reperfusion injury. *J Biol Chem*. 2004;279(33):34682-34690.

How to cite this article: Ayala S, Delco ML, Fortier LA, Cohen I, Bonassar LJ. Cartilage articulation exacerbates chondrocyte damage and death after impact injury. *J Orthop Res*. 2020;1–11. https://doi.org/10.1002/jor.24936